



ELSEVIER

Contents lists available at ScienceDirect

Comptes Rendus Chimie

www.sciencedirect.com



Full paper/Mémoire

Quantum chemical studies of non-covalent interactions between the ethyl cation and rare gases



Boaz G. Oliveira

Instituto de Ciências Ambientais e Desenvolvimento Sustentável, Universidade Federal da Bahia, 47801-100 Barreiras, BA, Brazil

ARTICLE INFO

Article history:

Received 22 July 2013

Accepted after revision 21 January 2014

Available online 1 August 2014

Keywords:

Ethyl cation

Rare gases

B3LYP

QTAIM

NBO

ABSTRACT

By taking into consideration the facts that rare gases (Ar, He, Kr, and Ne) are practically inert and that the structure of the ethyl cation ($C_2H_5^+$) is stabilized through the hyperconjugation effect, a theoretical study at the B3LYP/6-311++G(d,p) level of calculation was carried out here in order to investigate the formation of the $C_2H_5^+ \cdots Ar$, $C_2H_5^+ \cdots He$, $C_2H_5^+ \cdots Kr$, and $C_2H_5^+ \cdots Ne$ complexes. The charge transfers among H and Ar, He, Kr or Ne prove that the loss of electronic density on the rare gases are clearly noticeable. Additionally, the synergism between the structural changes and the vibration shifts have been demonstrated and justified on the basis of the Bent rule and QTAIM calculations. In complement, the interaction strength in $H^+ \cdots Ar$, $H^+ \cdots He$, $H^+ \cdots Kr$, and $H^+ \cdots Ne$ was examined, although the covalent character is completely null because these contacts are very weak.

© 2014 Académie des sciences. Published by Elsevier Masson SAS. All rights reserved.

1. Introduction

Nowadays, the studies of interatomic interactions have attained a level of complexity never seen before [1–5]. Besides dihydrogen bonds [6–10], halogen bonds [11–14], dihydride–halogen bonds [15–17], beryllium bonds [18], and pnictogen bonds [19,20], in general the electron flux on these interactions occur from high-electron-density centers, such as proton acceptors, towards the electron-depleted ones, which are represented by hydrogen donors [21–24]. Clearly, this electronic gearing controls the formation of these non-covalent links [25–27]. Anyhow, the research of new forms of intermolecular contacts is focused on the analysis of the high electron-density entity, because it is from the hyperconjugative interaction (charge transfer) [28] between the frontier molecular orbitals occurs. Otherwise, in some circumstances, hybridization (*ab initio* wave function) can manifest itself and outweigh hyperconjugation [29,30]. Actually, depending on the strength of the interaction, these two interpretative lines

rationalize the state-of-the-art to evaluate whether an intermolecular system is a stronger or a weaker bound.

Regarding proton donating in hydrogen bonding, it is known that they must not necessarily be neutral acids, and indeed, they can originate from ionic species. In agreement with this, it was established a very long time ago that some carbonium ions have the capability to acquire extra stability [31], but in this case, the occurrence of inconstant electronic fluxes plays a great role in the formation of electron-depleted molecular sites. If it happens, the carbocation may function as a proton donor, such as the ethyl cation ($C_2H_5^+$) does, for instance. Beyond being a typical representative of carbocations [32], $C_2H_5^+$ has been already examined and validated as a proton donor in the formation of hydrogen complexes with similar neutral molecules, such as acetylene, ethylene, as well as cyclopropane [33], wherein $\pi \cdots H$ hydrogen bonds appear. Moreover, $C_2H_5^+$ is also able to form dihydrogen bonds when it binds to magnesium hydride or beryllium hydride to form binary ($C_2H_5^+ \cdots MgH_2$ and $C_2H_5^+ \cdots BeH_2$) and ternary ($C_2H_5^+ \cdots 2MgH_2$ and $C_2H_5^+ \cdots 2BeH_2$) complexes [34,35].

Concerning the proton's acceptor nature, it is well known that molecules with lone pairs of electrons [36,37],

E-mail addresses: boazgaldino@gmail.com, boaz.galdino@ufob.edu.br.

unsaturated bonds [22,38] or even those with hydride groups [16,17] are able to receive acid protons. Otherwise, there is also another possibility of unusual proton receptors, for instance, the rare gases. In line with this, Cappelletti et al. [39] have stated the “birth of the hydrogen bond” between water and some rare gases, Barreto et al. [40] described van der Waals forces in complexes of water and peroxides with rare gases, whereas Jamshidi et al. [41] have asserted that metals and rare gases bind to each other in a stable form. Although the existence of protonated rare gas clusters is known [42], the main goal of the current work is focused on a quantum chemical study of intermolecular interactions between rare gases, such as argon, helium, krypton, or neon, and the ethyl cation ($C_2H_5^+$), whose $H\cdots Ar$, $H\cdots He$, $H\cdots Kr$, and $H\cdots Ne$ contacts will be examined by means of structural investigation, determination of electronic parameters, infrared spectroscopy analysis, topological integrations of charge densities, and molecular orbital calculations.

From a spectroscopic standpoint, the researches related to hydrogen bonds or any other similar interaction are currently performed on the basis of the s -(H) and p -(X) orbitals in the $H-X$ proton donor system (wherein X is more electronegative than hydrogen) [43], whose contributions as well as variations accord well with the Bent rule [44]. Being aware of this statement, the analysis of these orbitals should be one of the objectives to be fulfilled here because the Bent rule corroborates the hybridization theory and justifies the frequency shifts of the proton donors. As such, the shortening in the bond length of the proton donor is followed by a decrease in its polarity, by which an increase in the s -character of the orbital of X (within the $H-X$ molecule) is evidenced. If this occurs, displacements in the coordinates of H and X are expected, and surely this can be justified through the computation of their atomic radii by means of the Quantum Theory of Atoms in Molecules (QTAIM) [45]. Specifically, if the distance between these atoms is reduced, the relationship $\Delta r_H > \Delta r_X$ is valid. This inequality is related to the shortening of the bond length and with a blue shift in the stretch frequency [43]. On the other hand, if $\Delta r_H < \Delta r_X$, it means that a weakness in the proton donor bond is testified, which leads to an increase in the bond length, which, in turn, causes the appearance of a red shift in the $H-X$ oscillator [43].

On a purely theoretical viewpoint, these atomic radii are computed in the light of the QTAIM approach, with localization of Bond Critical Points (BCP) along each internuclear axis [46]. In addition, other topological properties are also determined, namely: electronic density (ρ), Laplacian ($\nabla^2\rho$), kinetic (G) and potential (U) electronic density energies. It is through the low and high values of ρ , the positive and negative ones of $\nabla^2\rho$, and finally if G outweighs U or vice-versa, that all $H\cdots RG$ (with $RG = Ar, He, Kr, \text{ and } Ne$) interactions and π bond of $C_2H_5^+$ are modeled. In practice, it is expected that the interaction strength profile of the $C_2H_5^+\cdots RG$ systems may be in good agreement with these kinds of analysis presented above, although it is widely known that the charge transfer mechanism still governs the formation of some intermolecular interactions [28,47–50], even if partially. Due to

this, the algorithms of the Charges from Electrostatic Potentials using a grid-based method (ChelpG) [51], Natural Bond Orbitals (NBO) [52], the traditional Mulliken population analysis [53], and naturally the QTAIM integrations [54] were applied during routine calculations. By these codes, the loss of atomic charge on the rare gases being transferred towards H, the phenomenon of shift in the frequency of the proton donor ($C_2H_5^+$), and of course the formation of the $H\cdots RG$ interaction can be certainly evidenced.

2. Computational procedure

The optimized geometries of the $C_2H_5^+\cdots RG$ complexes (with $RG = Ar, He, Kr, \text{ and } Ne$) were modeled at the B3LYP/6-311++G(d,p) level of theory. All calculations were carried out by the GAUSSIAN 98 W quantum software [55], by which the calculations of the ChelpG, NBO, and Mulliken atomic charges were also obtained. Moreover, the Boys and Bernardi function counterpoise method [56] implemented to eliminate the Basis Sets Superposition Error (BSSE) [57] and the Zero-Point vibrational Energy (ZPE) [58] were also included to correct the interaction energies. Regarding the QTAIM calculations, they were performed by AIMAll 11.05.16 software [59] after generation of the “*wfn*” archive by GAUSSIAN 98W.

3. Results and discussions

3.1. Structure and spectrum

Through the calculations performed at the B3LYP/6-311++G(d,p) level of theory, Fig. 1 illustrates the optimized geometries of the $C_2H_5^+\cdots Ar$ (I), $C_2H_5^+\cdots He$ (II), $C_2H_5^+\cdots Kr$ (III), and $C_2H_5^+\cdots Ne$ (IV) complexes. The distance values of 2.5822 (I), 2.4116 (II), 2.6126 (III), and 2.3956 Å (IV) for the $H\cdots RG$ interactions are shorter than the corresponding sum of the van der Waals radii [60–62], whose amounts are 2.97 ($H = 1.09 + Ar = 1.88$), 2.490 ($H = 1.09 + He = 1.40$), 3.11 ($H = 1.09 + Kr = 2.02$), and 2.63 Å ($H = 1.09 + Ne = 1.54$). In conformity with these assertions, but in view of the applicability in investigations of chemical bonds and interatomic distances [63,64], the interaction distance at the B3LYP/6-311++G(d,p) of I is shorter than the values reported by Goswami and Arunan [65] regarding the $H_2O\cdots 2Ar$ and $H_2S\cdots 2Ar$ complexes at the MP2(full)/aug-cc-pVTZ level of theory. Absolutely, this is not enough to discriminate the efficiency between these levels of theory, but otherwise it also serves to show that ternary structures have not necessarily shorter intermolecular distances and higher interaction energies compared with binary ones [21,27,66,67].

In addition to $H\cdots RG$, the values of the bond lengths of both $C\cdots H$ and π are also depicted in Fig. 1. Unlike many other intermolecular systems [68–70], the shorter interactions of II and IV are not responsible for the most intense molecular changes, in particular on the ethyl cation. Note that IV is a much shorter bound than III, although the corresponding values of Δr_π are -0.0006 and -0.0037 Å. Because the hyperconjugation controls the stabilization of

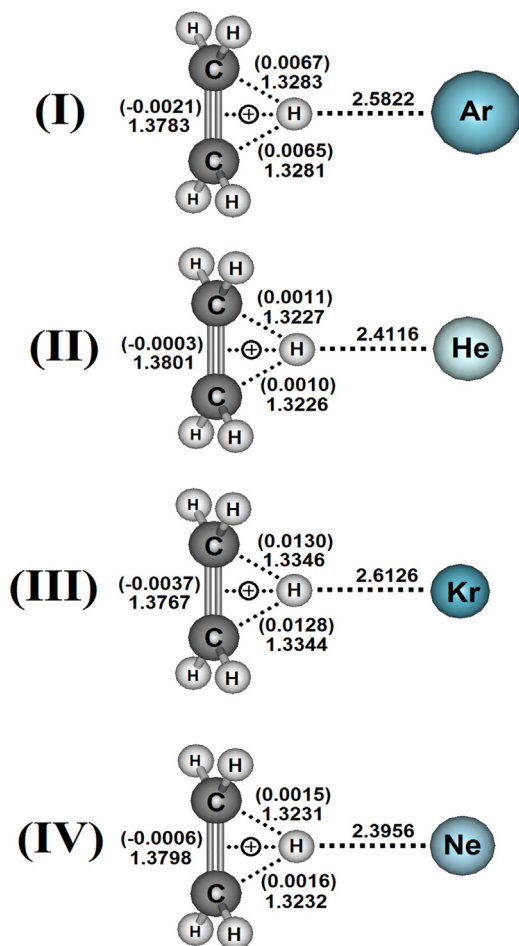


Fig. 1. (Color online.) Optimized geometries of the $C_2H_5^+ \cdots Ar$ (I), $C_2H_5^+ \cdots He$ (II), $C_2H_5^+ \cdots Kr$ (III), and $C_2H_5^+ \cdots Ne$ (IV) complexes obtained via B3LYP/6-311 + +G(d,p) calculations.

$C_2H_5^+$, this effect shows itself sensitive to the changes in the $\pi \cdots H$ and $C \cdots H$ contacts [71,72]. These bond lengths vary between 0.0199 and 0.0371 Å as well as between 0.0011 and 0.0130 Å; these profiles are not in line with the interaction strengths, obviously at this stage of the study regarding only the interatomic distances. However, all these results show a good concordance with the phenomenology of the infrared stretch modes, whose values are displayed in Table 1.

Although supported by the van der Waals radii, the long interatomic distances present weak stretch frequency modes, which oscillate between 62.8 and 89 cm^{-1} ; their absorption intensities are not so low (e.g., 30.88 and 42.70 $km \cdot mol^{-1}$ for II and III, respectively). As aforementioned, the π bonds are reduced and strengthened after the formation of the I–IV complexes, but now, the vibration analysis point out slight blue shifts with increasing absorption intensity ratios [73,74]. Bearing in mind that the ethyl cation is a proton donor, the distance shortening reaffirms that $\pi \cdots H$ possesses the same profile observed in a large number of systems stabilized via H-bond [75,76]. Similar to a selected group of systems [77,78], however,

Table 1

Values of the stretch frequencies and absorption intensities of the interatomic and molecular interactions as well as of the red- and blue shift effects of the I–II systems obtained through the B3LYP/6-311 + +G(d,p) level of theory.

IR modes	Interatomic and molecular systems			
	I	II	III	IV
$\nu_{H \cdots RG}$	80	68.10	89	62.8
$I_{H \cdots RG}$	30.88	6.21	42.7	16.9
$\nu_{\pi \cdots H,c}$	2093.1	2142.7	2035.9	2140.4
$\nu_{\pi \cdots H,m}$	2144.8 (2217) ^e	2144.8	2144.8	2144.8
$\Delta \nu_{\pi \cdots H}^a$	-51.7	-2.1	-108.9	-4.4
$I_{\pi \cdots H}$	179.2	55.73	338.9	67.88
$I_{\pi \cdots H}/I_{\pi \cdots H,m}^b$	4.1	1.3	7.8	1.6
ν_{π}	1574.4	1572.8	1575.6	1572.9
$\Delta \nu_{\pi}^c$	+1.8	+0.2	+3	0.3
I_{π}	19.99	10.4	34	11.2
$I_{\pi}/I_{\pi,m}^d$	2.1	1.01	3.6	1.2

Values of ν and I are given in cm^{-1} and $km \cdot mol^{-1}$, respectively.

^a $\Delta \nu_{\pi \cdots H} = \nu_{\pi \cdots H,c} - \nu_{\pi \cdots H,m}$ (complex - monomer), in which the value of $\nu_{\pi \cdots H,m}$ is 2144.8 cm^{-1} at the B3LYP/6-311 + +G(d,p) level of theory.

^b $I_{\pi \cdots H}/I_{\pi \cdots H,m}$, in which the value of $I_{\pi \cdots H,m}$ is 43 $km \cdot mol^{-1}$ at the B3LYP/6-311 + +G(d,p) level of theory.

^c $\Delta \nu_{\pi} = \nu_{\pi,c} - \nu_{\pi,m}$ (complex - monomer), in which the value of $\nu_{\pi,m}$ is 1572.63 cm^{-1} at the B3LYP/6-311 + +G(d,p) level of theory.

^d $I_{\pi}/I_{\pi,m}$, in which the value of $I_{\pi,m}$ is 9.47 $km \cdot mol^{-1}$ at the B3LYP/6-311 + +G(d,p) level of theory.

^e Experimental value: Ref. [80].

red and blue shifts also coexist in the ethyl cation. Just like mentioned by Yen et al. [79] in studies of complexes, such as $H-Ng-F \cdots H-F$ and $H-F \cdots H-Ng-F$, actually there is a synergism between $\Delta r_{\pi \cdots H}$ and $\Delta \nu_{\pi \cdots H}$, although all computed red shifts of -51.7 (I), -2.1 (II), -108.9 (III), and -4.4 cm^{-1} (IV) are not concordant with the profile of the interatomic strength. In other words, the intensities of the shifted frequencies are not affected by the interatomic distances. Note that the experimental value of 2217 cm^{-1} obtained by Duncan et al. [80] was satisfactorily reproduced by the value of 2144.8 cm^{-1} determined via B3LYP/6-311 + +G(d,p) calculations.

3.2. Energy and charge transfer: attraction, repulsion and eventual retro-donation

Some time ago, Salazar et al. [81] have mentioned the difficulty in studying complexes formed by rare gases. Especially about interaction energy, it is widely known that its quantity is negative if the geometry of the intermolecular complex falls at the minimum of the potential energy surface [82]. According to the values listed in Table 2, it can be perceived how I–IV complexes are weakly bound. As can be seen, the ΔZPE corrections outweigh BSSE, although in some cases, the BSSE values are negative [83], even though the interaction energy of -7.69 $kJ \cdot mol^{-1}$ reveals that III is the most stable complex. Contrary to what one might point out, intermolecular interactions with low energies are not unusual, as confirmed by a work by Lu et al. [84]. Of course, small BSSE amounts were also obtained, and above all else, this was also verified in weakly bound complexes modeled through the B3LYP/6-311 + +G(d,p) theoretical level [85]. Likewise, it may be highlighted that $H \cdots RG$ is a non-covalent interaction with low results of BSSE and ΔE^C ,

Table 2

Values of the interaction energies with corrections (ΔE^c with BSSE and ΔZPE included) and without corrections (ΔE determined by the energetic difference between complex and monomer) of the I–II systems obtained through the B3LYP/6-311 + G(d,p) level of theory.

Energies	Interatomic and molecular systems			
	I	II	III	IV
ΔE	-4.62	-0.61	-8.66	-2.21
BSSE	-0.40	0.02	-0.20	0.48
ΔZPE	1.29	0.93	1.17	1.07
ΔE^c	-3.73	+0.034	-7.69	-0.66

Values of ΔE , BSSE, ΔZPE , and ΔE^c are given in $\text{kJ}\cdot\text{mol}^{-1}$.

although this is not relevant because other intermolecular interactions also present a similar aspect [19]. What is quite clear in other works [86,87] is not evidenced here regarding the direct relationship between distances and energies of H...RG interactions.

One of the most applied procedures in the investigations of intermolecular interactions is the analysis of the charge-transfer mechanism, which has proven extremely efficient in several applications [88,89], although it is also neglected because the atomic charge has no physical basis and thereby is not included into the Schrödinger equation. Despite this, many are the algorithms implemented to compute atomic charges, namely those inserted into the ChelpG, NBO, Mulliken, and QTAIM schemes. From these approaches, Table 3 lists the values of the charge transfer ($\Delta Q_{\text{RG}}^{\text{ChelpG}}$, $\Delta Q_{\text{RG}}^{\text{NBO}}$, $\Delta Q_{\text{RG}}^{\text{Mull}}$, and $\Delta Q_{\text{RG}}^{\text{QTAIM}}$), whose mechanism was admitted as being initialized by donations of electronic density from rare gases towards the ethyl cation. In this manner, the positive values of ΔQ_{RG} reaffirm the transference of charge previously quoted, although it must be also asserted that the negative and small results of -0.00032 and 0.00088 au of II and IV are somewhat realistic because undoubtedly these systems are not only non-covalent but almost non-bonded. This scenario suggests that an electronic retro-donation from ethyl cation towards to neon and helium may be reliable.

Throughout the chemical literature with mention to hydrogen bonding [90,91], the great applicability of the charge transfers is concentrated in the characterization and/or justification of the shifting frequencies of the

proton donors when these species bind with high density centers [92]. By contrasting all amounts of $\Delta Q_{\text{RG}}^{\text{ChelpG}}$, $\Delta Q_{\text{RG}}^{\text{NBO}}$, $\Delta Q_{\text{RG}}^{\text{Mull}}$, and $\Delta Q_{\text{RG}}^{\text{QTAIM}}$ versus the values of $\Delta \nu_{\pi\cdots\text{H}}$, four relationships were equated as follows:

$$\Delta \nu_{\pi\cdots\text{H}} = -1277.5 \Delta Q_{\text{RG}}^{\text{ChelpG}} + 24.0, R^2 = -0.997 \quad (1)$$

$$\Delta \nu_{\pi\cdots\text{H}} = -3182.1 \Delta Q_{\text{RG}}^{\text{NBO}} + 6.75, R^2 = -0.999 \quad (2)$$

$$\Delta \nu_{\pi\cdots\text{H}} = -1639.5 \Delta Q_{\text{RG}}^{\text{Mull}} + 35.3, R^2 = -0.968 \quad (3)$$

$$\Delta \nu_{\pi\cdots\text{H}} = -3124.6 \Delta Q_{\text{RG}}^{\text{QTAIM}} - 0.8, R^2 = -0.993 \quad (4)$$

The role of charge transfer is well understood on the basis of the frontier molecular orbitals, in which the electron-density flows between them from the HOMO towards the LUMO of the proton acceptor and donor [93,94], respectively. Here, charge transfer is not entirely absolute because in the weakest bound systems, for instance II and IV, an electronic density retro-donation phenomenon (LUMO to HOMO) determined via QTAIM calculations is evidenced. Even though the linear and direct relationship between $\Delta Q_{\text{RG}}^{\text{NBO}}$ and $\Delta \nu_{\pi\cdots\text{H}}$ was established, Fig. 2 shows that NBO is an efficient approach in view of the linear coefficient of -0.999 .

3.3. NBO and QTAIM analysis: Bent rule and interaction strength

In a forward analysis of the molecular orbital, in Table 4 are listed other NBO parameters, such as the percentages of the *s*-character and *p*-character of carbon (π) and hydrogen (H...RG) in the ethyl cation. Increases of 0.03 and 0.09% as well as decreases of -0.02 and -0.01% in the *s*-character can be noted; these are closely related with the interaction strength of the I and III complexes as well as of the II and IV ones, respectively. For the first two complexes, which are the longer bound ones, conclusively the Bent rule is satisfied, whereas it is not for the last two complexes, because they are weakly bound and even energetically non-bonded. This analysis is not applied to interaction energy, but surely is treated as one additional

Table 3

Values of the charge transfers ($\Delta Q_{\text{RG}}^{\text{ChelpG}}$, $\Delta Q_{\text{RG}}^{\text{NBO}}$, $\Delta Q_{\text{RG}}^{\text{Mull}}$, and $\Delta Q_{\text{RG}}^{\text{QTAIM}}$) of the I–II systems obtained through the B3LYP/6-311 + G(d,p) level of theory.

Charges	Interatomic and molecular systems			
	I	II	III	IV
$\Delta Q_{\text{RG}}^{\text{ChelpG}}$	+0.063 (−0.088) [0.000]	+0.018 (−0.035) [+0.002]	0.102 (−0.131) [−0.001]	+0.023 (−0.042) [−0.003]
$\Delta Q_{\text{RG}}^{\text{NBO}}$	+0.019 (+0.002) [−0.006]	+0.0020 (+0.002) [−0.001]	+0.036 (+0.01) [−0.011]	+0.004 (+0.002) [−0.001]
$\Delta Q_{\text{RG}}^{\text{Mull}}$	+0.062 (−0.032) [−0.012]	+0.017 (−0.019) [−0.001]	+0.081 (−0.031) [−0.017]	+0.028 (−0.016) [−0.008]
$\Delta Q_{\text{RG}}^{\text{QTAIM}}$	+0.0183 (+0.006) [−0.005]	+0.0008 (+0.002) [−0.001]	+0.032 (+0.010) [−0.007]	−0.0003 (+0.007) [−0.0009]

Values of $\Delta Q_{\text{RG}}^{\text{ChelpG}}$, $\Delta Q_{\text{RG}}^{\text{NBO}}$, $\Delta Q_{\text{RG}}^{\text{Mull}}$, and $\Delta Q_{\text{RG}}^{\text{QTAIM}}$ are given in atomic units (au); values of charge transfer variation on H are given in parentheses; values of charge transfer variation on C are given in brackets.

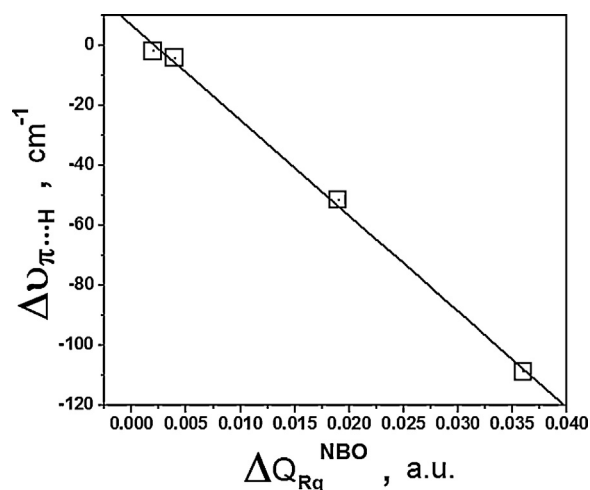


Fig. 2. Relationship between NBO charge transfer on rare gases (ΔQ_{Rg}^{NBO}) and red shifts on the $\pi \cdots H$ contact ($\Delta \nu_{\pi \cdots H}$).

Table 4

Values of the *s*- and *p*-characters of hydrogen and carbon in the **I–IV** systems obtained through the NBO analysis at the B3LYP/6-311++G(d,p) level of theory.

Hybridizations	Interatomic and molecular systems			
	I	II	III	IV
%s(C)	33.51	33.46	33.57	33.47
$\Delta\%s(C)^a$	0.03	-0.02	0.09	-0.01
%p(C)	66.32	66.38	66.28	66.37
$\Delta\%p(C)^b$	-0.04	0.02	-0.08	0.01
%s(H)	99.84	99.94	99.94	99.94
$\Delta\%s(H)^c$	-0.10	0.0	0.0	0.0
%p(H)	0.16	0.06	0.06	0.06
$\Delta\%p(H)^d$	0.1	0.0	0.0	0.0

All values designed above (subscripts a–d) were obtained at the B3LYP/6-311++G(d,p) level of theory.

^a $\Delta\%s(C) = \%s(C) - \%s(C)_{m}$, in which the values of $\%s(C)_{m}$ is 33.48;

^b $\Delta\%p(C) = \%p(C) - \%p(C)_{m}$, in which the values of $\%p(C)_{m}$ is 66.36;

^c $\Delta\%s(H) = \%s(H) - \%s(H)_{m}$, in which the values of $\%s(H)_{m}$ is 99.94;

^d $\Delta\%p(H) = \%p(H) - \%p(H)_{m}$, in which the values of $\%p(H)_{m}$ is 0.06.

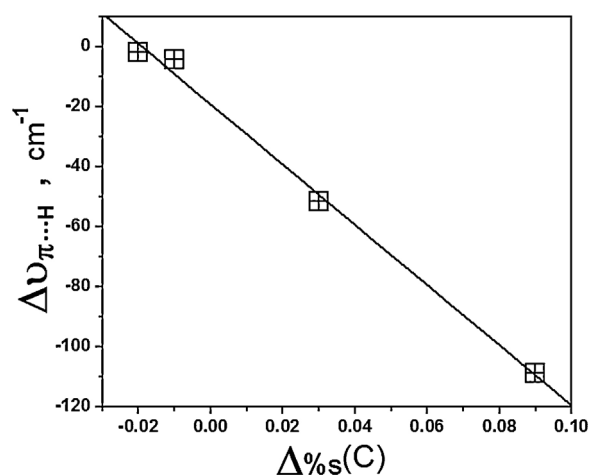


Fig. 3. Relationship between the red shifts on $\pi \cdots H$ contact ($\Delta \nu_{\pi \cdots H}$) and the variations of the *s*-character of the carbons ($\Delta \%s(C)$).

justification to the frequency shifts of the proton donors [43]. In this context, Fig. 3 illustrates the relationship between $\Delta \nu_{\pi \cdots H}$ and $\Delta \%s(C)$, whose linear profile with a coefficient of -0.997 yielded by the equation (5) can be considered highly satisfactory.

$$\Delta \nu_{\pi \cdots H} = -1004.18 \Delta \%s(C) - 19.18, R^2 = -0.997 \quad (5)$$

Another information must be registered regarding the blue shifts: the increase of $\%s(X)$ in X reinforces the characterization of the hybridization effect as dominant rather than the hyperconjugation upon the formation of the $Y \cdots H - X$ H-bond. So, hybridization would be present in stronger H-bond systems containing blue shifts on their proton donors [43]. Nevertheless, it should be pointed out that none of these events was identified here. On the contrary, this work presents a unanimous scenario with weakly bonded systems with interactions varying between 0.343 up to $-7.69 \text{ kJ} \cdot \text{mol}^{-1}$ followed by red shifts in the stretch frequencies of $\pi \cdots H$ proton donors oscillators.

In Tables 5–7 are organized several topological parameters (ρ , $\nabla^2 \rho$, G , U , $-G/U$, Δr^o , and ϵ) obtained from QTAIM calculations. In addition to the first four terms previously presented, other QTAIM parameters were introduced, such as Δr^o and ϵ . About Δr^o , it represents a measurement of the distance between the nucleus and the BCP along a bond path as well as how much this distance varies by the formation of the complex ($r_{\pi-BCP,c}^o$) in comparison with the monomer ($r_{\pi-BCP,m}^o$), which is often a proton donor in which the following subtraction is valid: $\Delta r_{\pi-BCP}^o = r_{\pi-BCP,c}^o - r_{\pi-BCP,m}^o$ [43]. In accordance with the hybridization theory, it was admitted that the manifestation of the blue shifts on proton donors would not be caused only by the increase in the *s*-character of the orbital of X (elements bound to H to form $H - X$) supported by the Bent rule, but the increase in the H radius compared with the value of X also reinforces this statement. Through the values of $\Delta r_{\pi-BCP}^o$ and Δr_{BCP-H}^o (see Table 5), the inference of $\pi \cdots H$ can be discussed, in which H is the proton donor site. In all complexes, QTAIM computation revealed that $\Delta r_{\pi-BCP}^o$ increases while Δr_{BCP-H}^o is reduced, meaning then $\Delta r_{\pi-BCP}^o > \Delta r_{BCP-H}^o$, which undoubtedly justifies the red-shift frequencies of -51.7 (I), -2.1 (II), -108.9 (III), and -4.4 cm^{-1} (IV).

Since we had a peculiar interest in assessing the subpart of the proton donor, blue shifts on the frequencies of the π bonds were identified in opposition to the red shifts of $\pi \cdots H$ discussed above. Due to the symmetry of the ethyl cation, the negative values of Δr_{C-C}^o (see Table 6) indicate a mutual movement of the carbon atoms toward the BCP located between them. Independently, the reductions of Δr_{C-C}^o are consistent with the blue shift results of $+1.8$ (I), $+0.2$ (II), $+3.0$ (III), and $+0.3 \text{ cm}^{-1}$ (IV). In agreement with the Bent rule [95], particularly the stronger bound complexes I and III are those in which the *s*-character of the carbon is enhanced. For the remaining complexes whose intermolecular stabilization is ruled by the lowest interaction energies, in other words as what has been observed in II and IV, there was no variation of the *s*-character of C and thereby the lowermost blue shift values of 0.2 – 0.3 cm^{-1} could not be explained.

Table 5
Values of the QTAIM properties of the $\pi\cdots\text{H}$ interactions in the I–IV systems.

Properties	Interatomic and molecular systems			
	I	II	III	IV
$\rho_{\pi\cdots\text{H}}$	0.0179 (–0.0018)	0.1809 (–0.0002)	0.1772 (–0.0039)	0.1808 (–0.0002)
$\nabla^2\rho_{\pi\cdots\text{H}}$	–0.2218 (–0.0027)	–0.2193 (–0.0005)	–0.2213 (–0.0026)	–0.2201 (–0.0014)
$G_{\pi\cdots\text{H}}$	0.0606 (–0.0022)	0.0625 (–0.0002)	0.0588 (–0.0039)	0.0622 (–0.0005)
$U_{\pi\cdots\text{H}}$	–0.1766 (0.0036)	–0.1798 (0.0004)	–0.1730 (0.0072)	–0.1795 (0.0007)
$-G/U_{(\pi\cdots\text{H})}$	0.3432	0.3400	0.3400	0.3470
$r_{\pi(\pi\cdots\text{H})}^{\rho}$	0.6947 (0.0095)	0.6863 (0.0011)	0.7034 (0.0182)	0.6872 (0.0020)
$r_{\text{H}(\pi\cdots\text{H})}^{\rho}$	0.4857 (–0.0018)	0.4874 (–0.0001)	0.4844 (–0.0032)	0.4872 (–0.0003)
$\epsilon_{\pi\cdots\text{H}}$	1.7873 (–0.0075)	1.8557 (–0.0071)	1.7189 (–0.1438)	1.8481 (–0.0147)

Values of ρ and $\nabla^2\rho$ are given in $\text{e}\cdot\text{a}_0^{-3}$ and $\text{e}\cdot\text{a}_0^{-5}$, respectively; values of G and U are given in electronic units (eu); values of r^{ρ} and Δr^{ρ} are given in angstroms (Å); variations are given in parentheses.

Table 6
Values of the QTAIM properties of the π bonds in the I–IV systems.

Properties	Interatomic and molecular systems			
	I	II	III	IV
ρ_{π}	0.3155 (0.0009)	0.3147 (0.0001)	0.3164 (0.0017)	0.3147 (0.00008)
$\nabla^2\rho_{\pi}$	–0.8909 (–0.0042)	–0.8871 (–0.0004)	–0.8955 (–0.0088)	–0.8867 (–0.00004)
G_{π}	0.1133 (0.0010)	0.1125 (0.0001)	0.1140 (0.0016)	0.1126 (0.0002)
U_{π}	–0.4495 (–0.0030)	–0.4468 (–0.0004)	–0.4519 (–0.0054)	–0.4469 (–0.0005)
$-G/U_{(\pi)}$	0.2522	0.2520	0.2520	0.2520
r_{π}^{ρ}	0.6906 (–0.0011)	0.6915 (–0.0002)	0.6898 (–0.0019)	0.6914 (–0.0003)
ϵ_{π}	0.1999 (0.0040)	0.1965 (0.0005)	0.2017 (0.0058)	0.1972 (0.0013)

Values of ρ and $\nabla^2\rho$ are given in $\text{e}\cdot\text{a}_0^{-3}$ and $\text{e}\cdot\text{a}_0^{-5}$, respectively; values of G and U are given in electronic units (eu); values of r_{π}^{ρ} are given in angstroms (Å); variations are given in parentheses.

Table 7
Values of the QTAIM properties of the $\text{H}\cdots\text{Rg}$ interactions in the I–IV systems.

Properties	Interatomic and molecular systems			
	I	II	III	IV
$\rho_{\text{H}\cdots\text{RG}}$	0.0098	0.0036	0.0126	0.0066
$\nabla^2\rho_{\text{H}\cdots\text{RG}}$	0.0300	0.0139	0.0328	0.0267
$G_{\text{H}\cdots\text{RG}}$	0.0060	0.0026	0.0068	0.0056
$U_{\text{H}\cdots\text{RG}}$	–0.0045	–0.0018	–0.0054	–0.0045
$-G/U_{(\text{H}\cdots\text{RG})}$	1.337	1.45	1.256	1.2300
$\epsilon_{\text{H}\cdots\text{RG}}$	0.0412	0.0430	0.0360	0.0452

Values of ρ and $\nabla^2\rho$ are given in $\text{e}\cdot\text{a}_0^{-3}$ and $\text{e}\cdot\text{a}_0^{-5}$, respectively; values of G and U are given in electronic units (eu).

Furthermore, it should be stressed that either the strengthening or the weakness of the π bond and $\pi\cdots\text{H}$ interaction can be interpreted in the light of the ellipticity (ϵ) [96,97], whose values are also displayed in Tables 5 and 6. Briefly speaking, it is well known that ϵ mimics the unsaturated character of the C–C bond in the 0.0–0.45 range (from ethane, benzene, up to ethylene) [46], indicating that the bond will be strengthened if the profile of ϵ is enlarged. Here, by focusing justly on π and $\pi\cdots\text{H}$, the ϵ values for these centers are enhanced and reduced after I–IV complexes have been formed. Because these events attest to stronger and weaker contacts, of course they can be also used as argument to justify the frequency changes, namely those shifted either to red or blue regions. As such, we plotted in Fig. 4, the relationship between the frequency shifts and ellipticity variations for π and

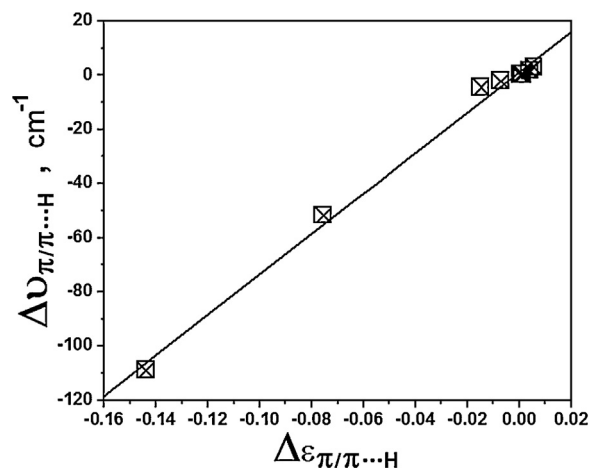


Fig. 4. Relationship between the frequency shifts and ellipticity variations of the π bonds and $\pi\cdots\text{H}$ contacts.

$\pi\cdots\text{H}$, and an excellent linear correlation was yielded by equation (6) below:

$$\Delta\nu_{\pi/\pi\cdots\text{H}} = 746.64 \Delta\epsilon_{\pi/\pi\cdots\text{H}} + 1.18, R^2 = 0.996 \quad (6)$$

One of the foundations of the QTAIM is devoted to the characterization (See Fig. 5) of BCPs (w , y , and z) and Bond Paths (BP) along the chemical bonds [98] (through the BCP pointed by w) and interatomic interactions (through the BCP pointed by z), in which it can be formed by low, median or high charge density concentrations [99–103]. Such designations can be predicted through the obtained

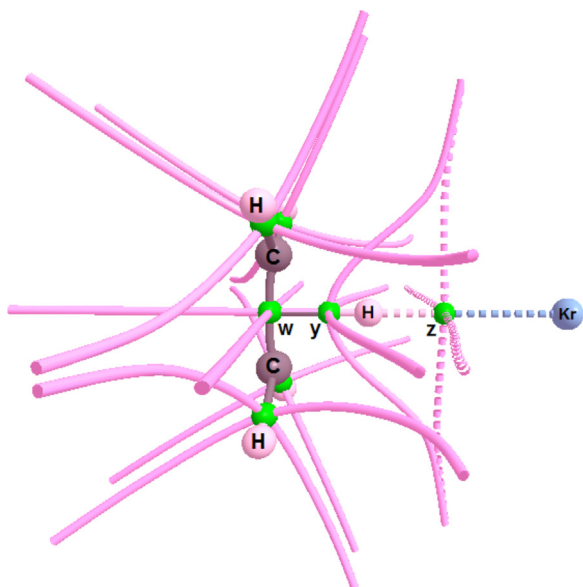


Fig. 5. (Color online.) Indication of the BCPs and BP for the $C_2H_5^+ \cdots Kr$ complex.

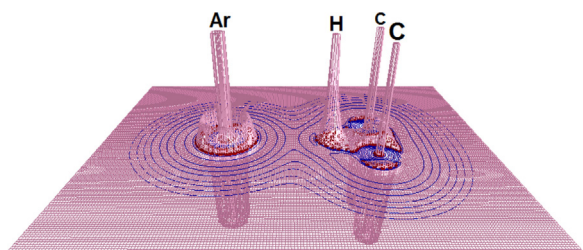


Fig. 6. (Color online.) Laplacian relief map of the $C_2H_5^+ \cdots Ar$ complex.

values of $\nabla^2\rho$ listed in Table 7 (the relief map of the $C_2H_5^+ \cdots Ar$ complex is illustrated in Fig. 6). It can be seen that the $\nabla^2\rho$ values for $H \cdots RG$ are positive, whereas they are negative for $\pi \cdots H$ and π (see Tables 5 and 6). In other words, the interaction $H \cdots RG$ is recognized as a closed-shell one and assumed to be non-covalent, albeit the very low energetic values have already revealed this before. In spite of this, the ratio values of G and U conduct the debate of the interaction strength as follows:

- $-G/U < 0.5$ indicates a total covalent character;
- $-G/U < 1.0$ indicates a partial covalent character;
- $-G/U > 1$ a non-covalent character [15,16,26].

Through this, it can be seen that all $H \cdots Rg$ interactions have no covalent character, whereas $\pi \cdots H$ and π are totally covalent. This scenario corroborates directly the slight frequency shifts and the low interaction energies.

Meanwhile, even though the interactive system is located in an energy minimum with low attraction strength, the prediction of its interaction strength is absolutely allowed, and it can be performed in conformity with the equation presented below [104,105]:

$$\Delta mol = [(\nu_0 - \nu/\nu_0)^2 + (\rho_0 - \rho/\rho_0)^2 + (\nabla^2\rho_0 - \nabla^2\rho/\nabla^2\rho_0)^2]^{1/2} \quad (7)$$

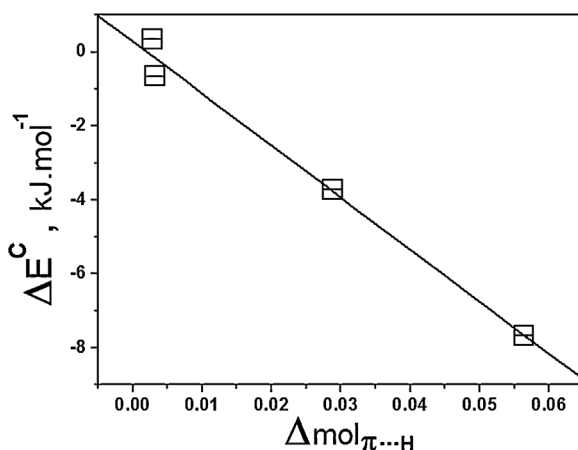


Fig. 7. Relationship between the interaction energies and the values of the $\Delta mol_{\pi \cdots H}$ parameter.

As a first result, the relationship between the interaction energies and the values of the Δmol parameter is graphically illustrated in Fig. 7, in which a linear coefficient of -0.994 was yielded by equation (8):

$$\Delta E^C = -141.08 \Delta mol_{\pi \cdots H} + 0.19, R^2 = -0.994 \quad (8)$$

In this, the vibration and topological properties used to generate the Δmol parameter were collected from the $\pi \cdots H$ contact. On the other hand, if the π bond is used instead of $\pi \cdots H$, the value of the linear coefficient of -0.988 obtained from the analysis of Fig. 8 is symbolized by equation (9):

$$\Delta E^C = -101.12 \Delta mol_{\pi} - 0.25, R^2 = -0.988 \quad (9)$$

Regarding the construction of these two models, vibration modes (red and blue shifts) were used instead of structural parameters [26], although it has been demonstrated that the vibration frequencies produce relationships well satisfactorily [104]. In any event, it should be emphasized that the ethyl cation disposes of two centers to predict the interaction strength with rare gases, namely the π bond and the $\pi \cdots H$ interaction.

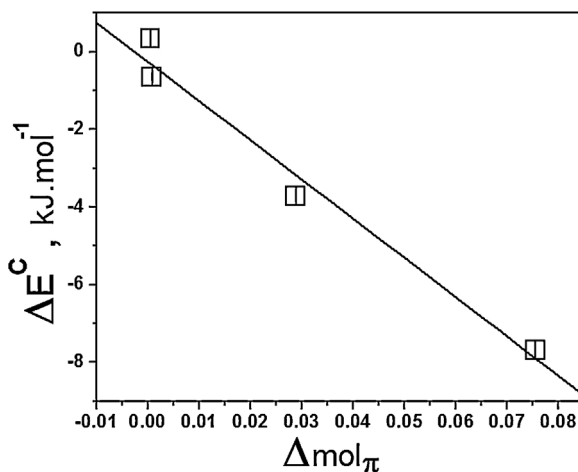


Fig. 8. Relationship between the interaction energies and the values of the Δmol_{π} parameter.

4. Conclusions

After a discerning discussion of geometry data, vibration modes, and electronic parameters of the $C_2H_5^+ \cdots Ar$, $C_2H_5^+ \cdots He$, $C_2H_5^+ \cdots Kr$ and $C_2H_5^+ \cdots Ne$ complexes, it can be affirmed that they are unusual intermolecular systems because the shifted frequencies of the π bonds and $\pi \cdots H$ contacts are partially supported by the hybridization orbital. About this, the $C_2H_5^+ \cdots Ar$ and $C_2H_5^+ \cdots Kr$ systems are stronger bound with interaction energies from -3.73 up to -7.69 $\text{kJ}\cdot\text{mol}^{-1}$, and thereby, they are fitted into the context of the Bent rule. The QTAIM calculations identified bond critical points and bond paths, wherein the high and low electronic densities followed by the negative and positive value of the Laplacian and electronic energy ratio (kinetic/potential) characterized π and $\pi \cdots H$ contacts as covalent, whereas the $H \cdots RG$ interaction as non-covalent. Moreover, the arising of blue and red shifts in π and $\pi \cdots H$ are accounted for by their strengthening and weakening, which can be explained via a decrease and an increase, respectively, in their values of ellipticity. The interpretation of the blue shifts is in line with the enhancements of the atomic radii of C computed by the QTAIM protocol, and in turn, reductions of the atomic radii of H are closely related to the appearance of the red shifts. At the end, even if $C_2H_5^+ \cdots He$ and $C_2H_5^+ \cdots Ne$ are weakly bound systems, the prediction of the interaction strength was successfully performed on the basis of vibration modes and of QTAIM parameters.

Acknowledgements

The author would like to thank to CNPq, CAPES and FAPESB Brazilian funding agencies.

Appendix A. Supplementary data

Supplementary data associated with this article can be found, in the online version, at <http://dx.doi.org/10.1016/j.crci.2014.01.014>.

References

- [1] G.A. Arteca, R.E. Cachau, K. Veluri, *Chem. Phys. Lett.* 319 (2000) 719–724.
- [2] S. Stadler, S. Hansen, I. Kröger, C. Kumpf, E. Umbach, *Nat. Phys.* 5 (2009) 153–158.
- [3] N. Pan, R.-Z. Wei, Y.-H. Chi, J.-M. Shi, W. Wei, Y.-Q. Zhang, *Z. Anorg. Allg. Chem.* 639 (2013) 1026–1031.
- [4] M.S. Gordon, Q.A. Smith, P. Xu, L.V. Slipchenko, *Ann. Rev. Phys. Chem.* 64 (2013) 553–578.
- [5] Z. Burghard, A. Leineweber, P.A. van Aken, T. Dufaux, M. Burghard, J. Bill, *Adv. Mater.* 25 (2013) 2468–2473.
- [6] B.G. Oliveira, R.C.M.U. Araújo, M.N. Ramos, *Spectrochim. Acta A* 68 (2007) 626–631.
- [7] B.G. Oliveira, R.C.M.U. Araújo, M.N. Ramos, *Struct. Chem.* 19 (2008) 185–189.
- [8] B.G. Oliveira, R.C.M.U. Araújo, M.N. Ramos, *Struct. Chem.* 19 (2008) 665–670.
- [9] B.G. Oliveira, R.C.M.U. Araújo, J.J. Silva, M.N. Ramos, *Struct. Chem.* 21 (2010) 221–228.
- [10] B.G. Oliveira, M.N. Ramos, *Int. J. Quantum Chem.* 110 (2010) 307–316.
- [11] B.G. Oliveira, R.C.M.U. Araújo, E.S. Leite, M.N. Ramos, *Int. J. Quantum Chem.* 111 (2011) 111–116.
- [12] P.-P. Zhou, W.-Y. Qiu, S. Liub, N.-Z. Jinc, *Phys. Chem. Chem. Phys.* 13 (2011) 7408–7418.
- [13] R. Wilcken, M.O. Zimmermann, A. Lange, A.C. Joerger, F.M. Boeckler, *J. Med. Chem.* 56 (2013) 1363–1388.
- [14] M.R. Scholfield, C.M.V. Zanden, M. Carter, P.S. Ho, *Protein Sci.* 22 (2013) 139–152.
- [15] M. Jabłoński, M. Palusiak, *J. Phys. Chem. A* 116 (2012) 2322–2332.
- [16] B.G. Oliveira, *Comput. Theor. Chem.* 998 (2012) 173–182.
- [17] B.G. Oliveira, *Phys. Chem. Chem. Phys.* 15 (2013) 37–79.
- [18] M. Yáñez, P. Sanz, O. Mó, I. Alkorta, J. Elguero, *J. Chem. Theory Comput.* 5 (2009) 2763–2771.
- [19] S. Scheiner, *J. Chem. Phys.* 134 (2011) 0932159–0943151.
- [20] J.E. Del Bene, I. Alkorta, G. Sánchez-Sanz, J. Elguero, *J. Phys. Chem. A* 116 (2012) 9205–9213.
- [21] B.G. Oliveira, R.C.M.U. Araújo, A.B. Carvalho, E.F. Lima, W.L.V. Silva, M.N. Ramos, A.M. Tavares, *J. Mol. Struct. (Theochem)* 775 (2006) 39–45.
- [22] B.G. Oliveira, R.C.M.U. Araújo, M.N. Ramos, A.B. Carvalho, *Struct. Chem.* 20 (2009) 663–670.
- [23] G.R. Desiraju, *Angew. Chem. Int. Ed.* 50 (2011) 52–59.
- [24] P. Goymer, *Nat. Chem.* 4 (2012) 863–864.
- [25] B.G. Oliveira, R.C.M.U. Araújo, A.B. Carvalho, M.N. Ramos, *J. Mol. Model.* 15 (2009) 421–432.
- [26] S.J. Grabowski, *Chem. Rev.* 111 (2011) 2597–2625.
- [27] B.G. Oliveira, R.C.M.U. Araújo, A.B. Carvalho, M.N. Ramos, *J. Mol. Model.* 17 (2011) 2847–2862.
- [28] B.G. Oliveira, R.C.M.U. Araújo, *Quim. Nova* 30 (2007) 791–796.
- [29] P.-P. Zhou, W.-Y. Qiu, N.-Z. Jin, *J. Chem. Phys.* 137 (2012) 084311–084315.
- [30] I.V. Alabugin, M. Manoharan, S. Peabody, F. Weinhold, *J. Am. Chem. Soc.* 125 (2003) 5973–5987.
- [31] J.E. Williams, V. Buss, L.C. Allen, *J. Am. Chem. Soc.* 93 (1971) 6867–6873.
- [32] H.-S. Andrei, N. Solc, O. Dopfer, *Angew. Chem. Int. Ed.* 47 (2008) 395–397.
- [33] B.G. Oliveira, M.L.A.A. Vasconcellos, R.R. Olinda, E.B.A. Filho, *Struct. Chem.* 20 (2009) 81–90.
- [34] B.G. Oliveira, M.L.A.A. Vasconcellos, *Inorg. Chem. Commun.* 12 (2009) 1142–1144.
- [35] B.G. Oliveira, M.L.A.A. Vasconcellos, *Struct. Chem.* 20 (2009) 897–902.
- [36] B.G. Oliveira, R.C.M.U. Araújo, A.B. Carvalho, M.N. Ramos, *J. Mol. Model.* 15 (2009) 123–131.
- [37] B.G. Oliveira, R.C.M.U. Araújo, A.B. Carvalho, M.N. Ramos, M.Z. Hernandez, K.R. Cavalcante, *J. Mol. Struct. (Theochem)* 802 (2007) 91–97.
- [38] B.G. Oliveira, R.C.M.U. Araújo, F.S. Pereira, E.F. Lima, W.L.V. Silva, A.B. Carvalho, M.N. Ramos, *Quim. Nova* 31 (2008) 1673–1679.
- [39] V. Aquilanti, E. Comicchi, M.M. Teixidor, N. Saendig, F. Pirani, D. Cappelletti, *Angew. Chem. Int. Ed.* 44 (2005) 2356–2360.
- [40] P.R.P. Barreto, F. Palazzetti, G. Grossi, A. Lombardi, G.S. Maciel, A.F.A. Vilela, *Int. J. Quantum Chem.* 110 (2010) 777–786.
- [41] Z. Jamshidi, K. Eskandari, S.M. Azami, *Int. J. Quantum Chem.* 113 (2013) 1981–1991.
- [42] F. Moncada, L.S. Uribe, J. Romero, A. Reyes, *Int. J. Quantum Chem.* 113 (2013) 1556–1561.
- [43] S.J. Grabowski, *J. Phys. Chem. A* 115 (2011) 12789–12799.
- [44] H.A. Bent, *Chem. Rev.* 61 (1961) 275–311.
- [45] R.F.W. Bader, *Atoms in Molecules – A Quantum Theory*, Oxford University Press, Oxford, UK, 1990.
- [46] R.F.W. Bader, *Chem. Rev.* 91 (1991) 893–928.
- [47] J. Goodman, L.E. Brus, *J. Chem. Phys.* 67 (1977) 4858–4865.
- [48] N. Gresh, P. Claverie, A. Pullman, *Int. J. Quantum Chem.* 29 (1986) 101–118.
- [49] R. Yerushalmi, A. Brandis, V. Rosenbach-Belkin, K.K. Baldrige, A. Scherz, *J. Phys. Chem. A* 110 (2006) 412–421.
- [50] D. Chaturvedi, V. Gupta, P. Tandon, A. Sharma, C. Baraldi, M.C. Gamberini, *Spectrochim. Acta A* 99 (2012) 150–159.
- [51] C.M. Breneman, K.B. Wiberg, *J. Comput. Chem.* 11 (1990) 361–373.
- [52] F. Weinhold, C.R. Landis, *Discovering Chemistry With Natural Bond Orbitals*, John Wiley & Sons, New Jersey, 2012.
- [53] R.S. Mulliken, *J. Chem. Phys.* 23 (1955) 1833–1840.
- [54] R.F.W. Bader, C.F. Matta, *J. Phys. Chem. A* 108 (2004) 8385–8394.
- [55] M.J. Frisch, G.W. Trucks, H.B. Schlegel, G.E. Scuseria, M.A. Robb, J.R. Cheeseman, J.A. Montgomery Jr., T. Vreven, K.N. Kudin, J.C. Burant, J.M. Millam, S.S. Iyengar, J. Tomasi, V. Barone, B. Mennucci, M. Cossi, G. Scalmani, N. Rega, G.A. Petersson, H. Nakatsuji, M. Hada, M. Ehara, K. Toyota, R. Fukuda, J. Hasegawa, M. Ishida, T. Nakajima, Y. Honda, O. Kitao, H. Nakai, M. Klene, X. Li, J.E. Knox, H.P. Hratchian, J.B. Cross, C. Adamo, J. Jaramillo, R. Gomperts, R.E. Stratmann, O. Yazyev, A.J. Austin, R. Cammi, C. Pomelli, J.W. Ochterski, P.Y. Ayala, K. Morokuma, G.A.

- Voth, P. Salvador, J.J. Dannenberg, V.G. Zakrzewski, S. Dapprich, A.D. Daniels, M.C. Strain, O. Farkas, D.K. Malick, A.D. Rabuck, K. Raghavachari, J.B. Foresman, J.V. Ortiz, Q. Cui, A.G. Baboul, S. Clifford, J. Cioslowski, B.B. Stefanov, G. Liu, A. Liashenko, P. Piskorz, I. Komaromi, R.L. Martin, D.J. Fox, T. Keith, M.A. Al-Laham, C.Y. Peng, A. Nanayakara, M. Challacombe, P.M.W. Gill, B. Johnson, W. Chen, M.W. Wong, C. Gonzalez, J.A. Pople, Gaussian, Gaussian, Inc, Pittsburgh PA, 2003.
- [56] S.F. Boys, F. Bernardi, *Mol. Phys.* 19 (1970) 553–566.
- [57] F.B. Van Duijneveldt, J.G.C.M. van Duijneveldt-van de Rijdt, J.H. van Lenthe, *Chem. Rev.* 94 (1994) 1873–1885.
- [58] A. Ruzsinszky, C. Van Alsenoy, G.I. Csonka, *J. Phys. Chem. A* 107 (2003) 736–744.
- [59] T.A. Keith, AIMAll Version 11.05.16, 2011.
- [60] A. Bondi, *J. Phys. Chem.* 68 (1964) 441–451.
- [61] R.S. Rowland, *J. Phys. Chem.* 100 (1996) 7384–7391.
- [62] S. Alvarez, *Dalton Trans.* 42 (2013) 8617–8636.
- [63] H. Böhm, R. Ahlrichs, *J. Chem. Phys.* 77 (1982) 2028–2034.
- [64] G.P. Schiemenz, *Z. Naturforsch.* 62b (2007) 235–243.
- [65] M. Goswami, E. Arunan, *Phys. Chem. Chem. Phys.* 11 (2009) 8974–8983.
- [66] B.G. Oliveira, R.C.M.U. Araújo, *J. Mol. Model.* 18 (2012) 2845–2854.
- [67] B.G. Oliveira, R.C.M.U. Araújo, F.F. Chagas, A.B. Carvalho, M.N. Ramos, *J. Mol. Model.* 14 (2008) 949–955.
- [68] B. Makiabadi, M. Zakarianejad, S. Bagheri, H.R. Masoodi, R.S. Aghaie, *Int. J. Quantum Chem.* 113 (2013) 2361–2371.
- [69] S. Scheiner, *Acc. Chem. Res.* 46 (2013) 280–288.
- [70] B.G. Oliveira, R.C.M.U. Araújo, *Can. J. Chem.* 90 (2012) 368–375.
- [71] J.J. Dannenberg, T.D. Berke, *Theor. Chem. Acc.* 24 (1972) 99–101.
- [72] P.D.B. de la Mare, *Pure Appl. Chem.* 56 (1984) 755–1766.
- [73] B.G. Oliveira, R.C.M.U. Araújo, M.N. Ramos, *J. Mol. Struct. (Theochem)* 908 (2009) 79–83.
- [74] B.G. Oliveira, R.C.M.U. Araújo, M.N. Ramos, *J. Mol. Struct. (Theochem)* 944 (2010) 168–172.
- [75] P. Hobza, Z. Havlas, *Chem. Rev.* 100 (2000) 4253–4264.
- [76] I.V. Alabugin, M. Manoharan, F.A. Weinhold, *J. Phys. Chem. A* 108 (2004) 4720–4730.
- [77] W. Yu, Z. Lin, Z. Huang, *ChemPhysChem.* 7 (2006) 828–830.
- [78] B.G. Oliveira, M.C.A. Lima, I.R. Pitta, S.L. Galdino, M.Z. Hernandez, *J. Mol. Model.* 16 (2010) 119–127.
- [79] S.-Y. Yen, C.-H. Mou, W.-P. Hu, *Chem. Phys. Lett.* 383 (2004) 606–611.
- [80] A.M. Ricks, G.E.P. Douberly, V.R. Schleyer, M.A. Duncan, *Chem. Phys. Lett.* 480 (2009) 17–20.
- [81] M.C. Salazar, J.L. Paz, A.J. Hernández, C. Manzanara, E.V. Ludeña, *Int. J. Quantum Chem.* 95 (2003) 177–183.
- [82] Z. Latajka, S. Scheiner, *J. Chem. Phys.* 87 (1987) 1194–1204.
- [83] P. Salvador, M.M. Szcześniak, *J. Chem. Phys.* 118 (2003) 537–549.
- [84] Y. Lu, H. Li, X. Zhu, H. Liu, W. Zhu, *Int. J. Quantum Chem.* 112 (2012) 1421–1430.
- [85] M.C. Daza, J.A. Dobado, J.M. Molina, P. Salvador, M. Duran, J.L. Villaveces, *J. Chem. Phys.* 110 (1999) 11806–11813.
- [86] P.S. Kushawaha, P.C. Mishra, *Int. J. Quantum Chem.* 76 (2000) 700–713.
- [87] I. Mata, I. Alkorta, E. Espinosa, E. Molins, *Chem. Phys. Lett.* 507 (2011) 185–189.
- [88] A. Vogler, H. Kunkely, *Coord. Chem. Rev.* 208 (2000) 321–329.
- [89] T. Kubař, M. Elstner, *J. Phys. Chem. B* 112 (2008) 8788–8798.
- [90] J.M. Herbert, M. Head-Gordon, *J. Am. Chem. Soc.* 128 (2006) 13932–13939.
- [91] S.G. Ramesh, S. Re, J.T. Hynes, *J. Phys. Chem. A* 112 (2008) 3391–3398.
- [92] A.M. Wright, A.A. Howard, J.C. Howard, G.S. Tschumper, N.I. Hammer, *J. Phys. Chem. A* 117 (2013) 5435–5446.
- [93] E. Ramos-Cordoba, D.S. Lambrecht, M. Head-Gordon, *Faraday Discuss.* 150 (2011) 345–362.
- [94] V. Balachandran, G. Mahalakshmi, A. Lakshmi, A. Janaki, *Spectrochim. Acta A* 97 (2012) 1101–1110.
- [95] S. Noorizadeh, *J. Mol. Struct. (Theochem)* 713 (2004) 27–32.
- [96] K. Durka, R. Kamiński, S. Luliński, J. Serwatowski, K. Woźniak, *Phys. Chem. Chem. Phys.* 12 (2010) 13126–13136.
- [97] R.N. Singh, V. Baboo, P. Rawat, V.P. Gupta, *J. Mol. Struct.* 1037 (2013) 338–351.
- [98] R.F.W. Bader, *J. Phys. Chem. A* 113 (2009) 10391–10396.
- [99] B.G. Oliveira, M.L.A.A. Vasconcelos, *J. Mol. Struct. (Theochem)* 774 (2006) 83–88.
- [100] E.B.A. Filho, E. Ventura, S.A. do Monte, B.G. Oliveira, C.G.L. Junior, G.B. Rocha, M.L.A.A. Vasconcelos, *Chem. Phys. Lett.* 449 (2007) 336–340.
- [101] B.G. Oliveira, L.F.C.C. Leite, *J. Mol. Struct. (Theochem)* 915 (2009) 38–42.
- [102] B.G. Oliveira, R.C.M.U. Araújo, *Monatsh. Chem.* 142 (2011) 861–873.
- [103] B.G. Oliveira, R.C.M.U. Araújo, M.N. Ramos, *Quim. Nova* 33 (2010) 1155–1162.
- [104] B.G. Oliveira, F.S. Pereira, R.C.M.U. de Araújo, M.N. Ramos, *Chem. Phys. Lett.* 427 (2006) 181–184.
- [105] B.G. Oliveira, R.C.M.U. de Araújo, M.N. Ramos, *Chem. Phys. Lett.* 433 (2007) 390–394.